Emplacement of giant radial dikes in the northern Tharsis region of Mars

Evelyn D. Scott
Environmental Science Department, Institute of Environmental and Natural Sciences, Lancaster University, Lancaster, UK

Lionel Wilson
Environmental Science Department, Institute of Environmental and Natural Sciences, Lancaster University, Lancaster, UK

Department of Geological Sciences, Brown University, Providence, Rhode Island, USA

James W. Head III
Department of Geological Sciences, Brown University, Providence, Rhode Island, USA

Received 24 November 2000; revised 30 August 2001; accepted 9 October 2001; published 13 April 2002.

[1] Three distinct sets of graben are associated with the volcano Alba Patera on Mars. One set, approximately circumferential to the edifice, has long been accepted to have formed as a tectonic response to an extensional stress regime associated with the evolution of the Alba Patera edifice. A second set includes mainly linear structures interpreted by many workers to have formed in response to very large-scale regional stresses. We infer that the third set of graben, all of which are relatively linear, none of which are strictly parallel to members of the second set, and many of which contain numerous pit craters, formed above long (~1000 km), laterally propagating regional dikes emanating from a volcanic center located to the south within the Tharsis region. The expected geometries of such dikes (several hundred meters depth to dike top, ~20 km depth to dike base, mean dike width ~30–90 m) are modeled on the assumption that they were fed from a shallow magma reservoir centered on a neutral buoyancy horizon, expected to be present at a depth of ~10 km on Mars. The volumes of magma in the dikes are consistent with a reservoir similar in size to those inferred to be present under the Tharsis shield volcanoes provided that the dikes were emplaced during caldera collapse episodes. The sizes of the graben associated with these dikes are consistent with the relaxation, during or immediately after dike emplacement, of preexisting regional extensional stresses of a few tens of MPa. *INDEX TERMS:* 8450 Volcanology: Planetary volcanism (5480); 8434 Volcanology: Magma migration; 5475 Planetology: Solid Surface Planets: Tectonics (8149); 6225 Planetology: Solar system objects: Mars; *KEYWORDS:* Mars, Tharsis, dike, graben

1. Introduction

[2] Alba Patera is a very large, low-relief shield volcano located on the northern flanks of the Tharsis Plateau, Mars. With a diameter of ~2700 km [*Cattermole*, 1996, p. 285] and a maximum topographic altitude of 6769 m [*Head et al.*, 1998; *Smith et al.*, 2001] its shape contrasts markedly with that of the other shield volcanoes of the Tharsis province: the Olympus, Arsia, Ascraeus, and Pavonis Montes are typically ~600 km in diameter and more than ~15 km in elevation [*Cattermole*, 1996, p. 268; *Smith et al.*, 2001]. The Alba Patera edifice is almost completely surrounded by numerous graben (Figure 1). These are approximately circumferential to the summit caldera to the west and east but join the approximately N-S trend of regional graben, found throughout Tharsis, to the south and partly merge into (and partly cut across) a NE-SW trending set of regional graben to the north. The graben at Alba Patera have been analyzed in detail by *Tanaka* [1990], who identified four stages of faulting. It is a subset of Tanaka's stage IV graben, formed at the end of the active life of Alba Patera, that is discussed in this paper.

[3] The graben approximately circumferential to the summit caldera of Alba Patera are a tectonic response either to the loading of the volcano onto the lithosphere [*Turtle and Melosh*, 1997] or to uplift following late-stage underplating of hot material [*McGovern et al.*, 1999; *Scott*, 2000a, 2000b]. These graben crosscut both lava flows and fluvial channels on the northern flanks of Alba Patera [*Turtle and Melosh*, 1997] and thus developed after the cessation of significant volcanic activity there. The graben to the north and south of Alba are interpreted by *Tanaka* [1990] to be the expression of more regional extensional stress systems.

[4] A third set of graben is associated with Alba Patera; these are contemporaneous with *Tanaka*'s [1990] stage IV graben but strike obliquely to both of the systems described above (Figure 1). They contain numerous chains of rimless pit craters (Figure 2), for which *Scott and Wilson* [2002] propose a volcanic origin, resulting from either the escape of gas which had accumulated at the top of a dike or the large-scale explosive eruption of dike magma. For convenience, we subsequently refer to these graben as "volcanic" graben and to the other graben systems as "tectonic" graben. We concur with *Mège and Masson* [1996a] in associating these graben with long, regional dikes. *Tanaka and Golombek* [1989] discuss the roughly NE-SW trending sets of graben with pit chain craters on the east side of Alba and identify a possible common origin from which graben-related dikes radiate within the northern flanks of Ascraeus Mons at 104°W, 22°N. We have identified additional graben with pit chain craters to the west of Alba (Figure 1), where they trend

0148-0227/02/2000JE001431$09.00

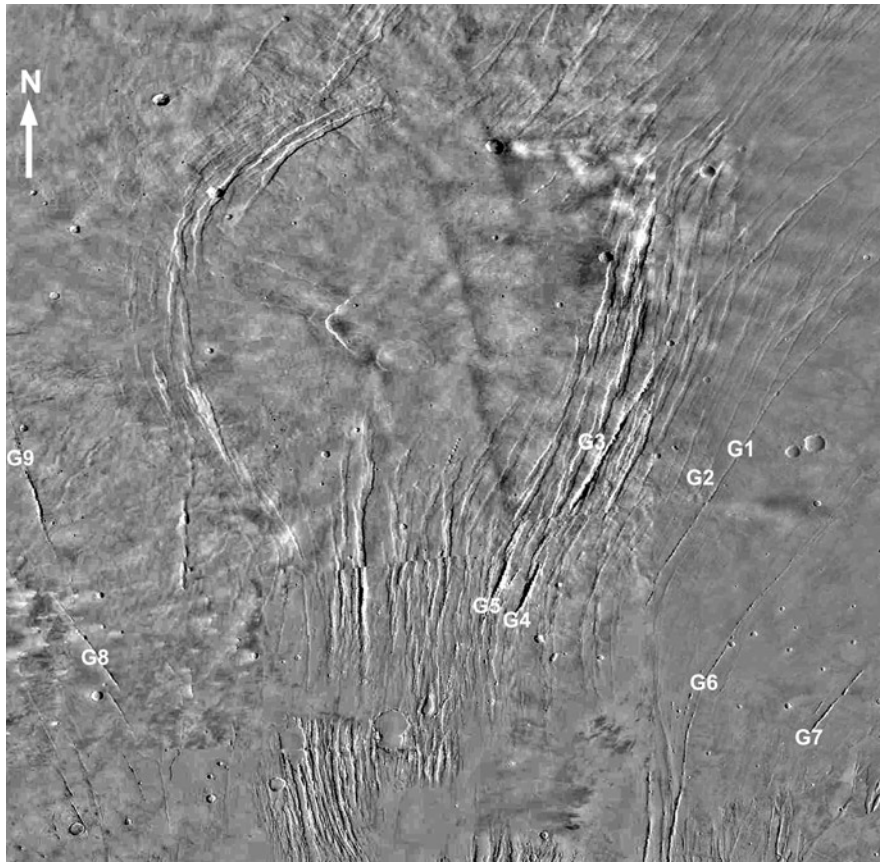

Figure 1. Viking image mosaic (Mercator projection) of the Alba Patera region (27.5°–47.5°N, 97.5°–117.5°W) from http://pdsmaps.wr.usgs.gov/. The many approximately circumferential graben are recognized by several previous authors as being due to extensional forces acting mainly radial to the edifice. The relatively linear graben trending approximately NE-SW to the north of Alba and N-S to the south of Alba are due to regional extensional stresses. This study focuses on the linear graben with associated pit craters, labeled G1–G9, which we infer to have formed as a result of surface extension related to the intrusion of giant dikes radial to a center to the south of the region.

NW-SE, and infer that the entire set converges toward a location farther south within the Tharsis Volcanic Province. Given the locations of the graben and the great distance, at least ~1000 km, to the source of the dikes, the source position cannot be determined accurately.

[5] Terrestrial regional dike swarms associated with flood basalt volcanism, such as the Mackenzie dike swarm in Canada, can be at least 2000 km long [*Ernst et al.*, 1995], more than twice the length of these Martian examples. However, Martian dikes are expected to be able to propagate farther from source reservoirs than their terrestrial counterparts because the smaller Martian gravity causes them to have greater widths [*Wilson and Parfitt*, 1990] and this increases the flow speed and reduces the cooling of magma within them [*Wilson and Head*, 1994]. Other graben systems associated with dikes in southern Tharsis extend for more than 2000 km [*Wilson and Head*, 2002], and so the Martian examples under study here should not be regarded as exceptional.

[6] In section 2 of this paper we present the geometric properties of some of the volcanic graben and discuss the relationships between the morphologies of the graben and their inferred underlying dikes. In section 3 we develop a model predicting the vertical extents and widths of giant radial dikes propagating from crustal magma reservoirs on Mars. In section 4 we discuss the significance of the fact that the model predicts dike widths significantly smaller than those inferred from the graben properties and use this to make inferences about the state of regional stress at the time the dikes were emplaced. Finally, in section 5 we draw some conclusions about the nature of the magma reservoir which would be required to explain the presence of the giant dikes.

2. Physical Parameters of the Volcanic Graben and the Inferred Giant Dikes

[7] Three of the volcanic graben cutting the flanks of Alba Patera, designated G1, G2, and G3 in Figure 1, were analyzed in detail, and their basic geometric properties (length, width, and depth) are given in Table 1, which also shows the Viking Orbiter frame numbers from which data were gathered. The lengths of the graben extrapolated from the intersection point of the eastern and western sets are up to 1000 km (Figure 1), and their widths range from ~2 to ~10 km. Depths were found mainly from measured shadow lengths using solar elevations from the PDS database at http://www-pdsimage.jpl.nasa.gov/cgi-bin/msearch.pl. In a few places, Mars Orbiter Laser Altimeter (MOLA) [*Smith et al.*, 1998] tracks from the Mars Global Surveyor spacecraft crossed the graben and provided more accurate values. The depths mainly lie in the range 80–350 m with means of 105, 110, and 350 m for graben G1, G2, and G3, respectively. If the boundary faults of the graben dip at 60° [*Golombek et al.*, 1996], the horizontal extensions across the three graben are ~120, 125, and 405 m, respec-

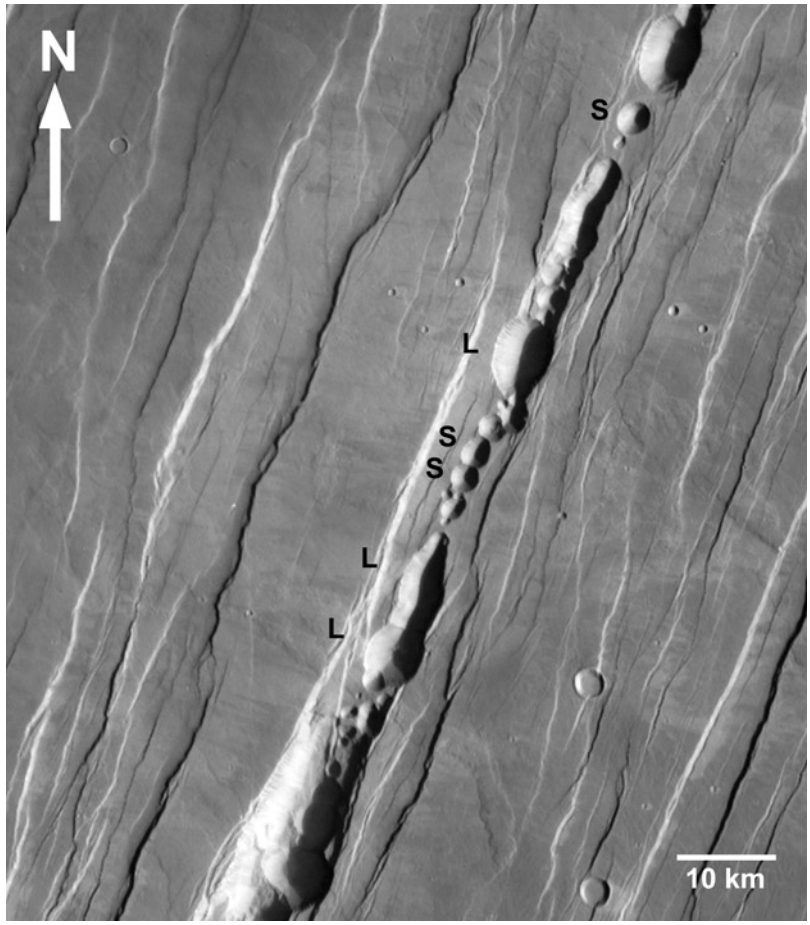

Figure 2. Examples of the pit craters associated with some linear graben near Alba Patera. We infer that the smaller craters (examples labeled S) formed by collapse after release of magmatic volatiles along the graben boundary faults; the larger craters (examples labeled L) sometimes have marginally raised rims and may be the results of violent basaltic plinian eruptions which excavated significant amounts of material from the dikes and dispersed them over very large areas as fall deposits from high eruption clouds. This image also shows an intersection between volcanic and tectonic graben. Viking Orbiter image 254s09.

tively. If the dips of the boundary faults are steeper, as is likely if they initiate at the surface and propagate downward, an average dip of 70°–75° may be more appropriate [*Mège and Masson*, 1996b], implying much smaller extensions of ~65, 70, and 220 m, respectively. These values are summarized in Table 1.

[8] The simplest possible interpretation of these extensions is that they represent estimates of the widths of the underlying dikes. This would be true if the dike intrusion and graben formation events shared a common cause, relaxation of a regional extensional stress. However, as we noted in section 1, the graben under study here do not exactly follow the orientations of any of the other graben in the region. This strongly suggests that the regional stress field in existence prior to dike emplacement is not the only factor controlling the emplacement; instead, a combination of the magma pressure distribution in the dike and the influence of the local host rock stress field controls both the dike orientation and the formation of the overlying graben. The nature of the control on graben formation is imperfectly understood, however. Owing to the

Table 1. Data Sources for the Three Volcanic Graben, G1–G3 in Figure 1, Analyzed in Detail, Measured Widths and Depths of Graben, Calculated Extensions Across Graben, and Inferred Properties of Underlying Dikes[a]

Grabel Label	Viking Orbiter Frames	Graben Width, m	Graben Depth, m	Graben Extension, m	Depth to Dike Top, m	Dike Width, m
G1	254s41, 43, 46, 48	2,300	105	65–120	650	130
G2	254s17, 19, 21, 24	3,600	110	70–125	1,000	140
G3	253s45, 47, 49, 52, 54	10,000	350	220–405	2,900	440

[a] See text for discussion.

requirement that a specific narrow vertical part of the sequence be exposed to observe the relationship between dike tips and faults, only a few direct exposures of graben directly associated with dikes are reported in the literature for the Earth [e.g., *Gudmundsson*, 1983]. This problem is exacerbated by the fact that the closest terrestrial analogs to the large Martian dikes inferred here are Archean giant dike swarms [*Ernst et al.*, 1995] for which the surface and near-surface expressions are particularly poorly preserved in the geologic record. However, evidence indicating that graben formation has accompanied dike emplacement includes eruption features (cones and domes) [*Head and Wilson*, 1993] and magnetic anomolies [*Srnka et al.*, 1979] aligned with lunar graben, and the radial orientation of graben well beyond the influence of regional stresses on Mars [*Wilson and Head*, 2002].

[9] *Rubin* [1992] inferred a connection between dikes and graben at two locations in Iceland and applied a theoretical model which included inelastic displacements on boundary faults to evaluate the ratios between (1) graben width and depth of dike top below the surface and (2) dike width and graben depth. He found graben width to dike top depth ratios of 4 in one case and 2.9 in another and corresponding dike width to graben subsidence ratios of 1.0 and 1.5. These values are within a factor of 2 of the results of analog laboratory modeling experiments by *Mastin and Pollard* [1988] to produce graben structures above intrusions. Although these analog models cannot readily be scaled to field conditions, the agreement with Rubin's values is remarkably close. If we adopt *Rubin*'s [1992] average value of ~3.5 for the graben width to dike top depth ratio, the measured mean widths of the Martian graben G1, G2, and G3 (2.3, 3.6, and 10 km, respectively) would imply that the dikes producing them had their tops at depths of ~0.65, 1.0, and 2.9 km. *Rubin*'s [1992] mean ratio of dike width to amount of vertical graben subsidence, ~1.25, would imply that our measured graben depths of 105, 110, and 350 m correspond to mean dike widths of ~130, 140, and 440 m for the dikes underlying graben G1, G2, and G3, respectively. These values are summarized in Table 1. The dike widths inferred in this way are a factor of 2 larger than those implied by adopting the strain across the graben as the dike width estimate, and this discrepancy is probably a realistic expression of current uncertainty in relating graben formation to dike emplacement. The implications of this are discussed in section 4.

[10] The widths of the graben we are studying are very uniform, and their horizontal lengths are very great. If, as we infer, they are linked directly to shallow dike intrusion from a reservoir located at the intersection of the systems to the west and east of Alba Patera, the dikes must be propagating laterally from the magma source in much the same way that, on a much smaller scale, dikes propagate in shield volcano rift zones [*Rubin and Pollard*, 1987], with the top and bottom of the dike trapped by the combination of internal magma pressure and external host rock stresses. In section 3 we develop a model of a laterally propagating dike linked to a pressurized magma reservoir and use this to predict the dike width and the depth to dike top for comparison with the above estimates.

3. Pressures and Stress Conditions in Radial Dikes and Their Magma Reservoir Sources

[11] In order to assess the consequences of models of magma reservoirs and dikes emanating from them, we assume that the centers of the dikes and the reservoir will be located at a neutral buoyancy level, where the magma density and that of the aggregate country rock are approximately equal [*Ryan*, 1987]. The Tharsis province on Mars, within which the features considered here are located, appears to have been dominated by mafic volcanism over a large part of the history of the planet [*Hodges and Moore*, 1994]. We therefore use the model developed by *Head and Wilson* [1992] to characterize the variation with depth of density and lithostatic stress in areas consisting of accumulating mafic volcanic rocks in which there is a finite average pore space at the surface which is progressively reduced by the increasing vertical stress with increasing depth. The density ρ_l and stress P_l are given as a function of the depth z below the surface by

$$\rho_l = \rho_\infty / \{1 + [V_0/(1 - V_0)\exp(-\lambda \rho_\infty g z)]\}, \quad (1)$$

$$P_l = P_{atm} + \lambda^{-1} \ln[V_0 + (1 - V_0)\exp(\lambda \rho_\infty g z)], \quad (2)$$

where V_0 is the volume fraction of the surface rocks that consists of void space; λ is a constant, independent of the acceleration due to gravity, g, that characterizes the exponential decay of void space with increasing pressure; ρ_∞ is the density of the lithospheric rocks at great depths where all of the void space has been removed; and P_{atm} is the atmospheric pressure. We assume $V_0 = 0.3$, a little larger than the 0.25 more typical of basaltic eruptives on Earth, to allow for the likely greater vesicularity of lavas on Mars [*Wilson and Head*, 1994]. We use $\lambda = 1.18 \times 10^{-8}$ Pa^{-1}, the value found for volcanic rocks in Hawai'i and Iceland [*Head and Wilson*, 1992]; take $g = 3.74$ m s^{-2} and $P_{atm} = 600$ Pa at the mean Martian datum; and adopt $\rho_\infty = 2900$ kg m^{-3} for void-free solid basaltic rocks. Using these values, the bulk density of the surface rocks is 2175 kg m^{-3}. A reasonable liquid basalt density corresponding to a void-free solid basalt density of 2900 kg m^{-3} is $\rho_{ml} = 2600$ kg m^{-3} [*Rubin and Pollard*, 1987], and (1) shows that the lithosphere reaches this density at a depth of 10.3 km, which is therefore the level of neutral buoyancy. The lithostatic pressure at this depth is given by (2) as 90.3 MPa. Note that these figures are based on the assumption that the geochemistry of the country rocks and the magma within the dikes are all basaltic. Pathfinder analyses of the rocks at the mouth of the Ares Valles indicate that they are very similar to Icelandic anorogenic andesites [*Golombek*, 1998; *McSween et al.*, 1999]. Changing the densities to be consistent with this has a negligible effect on the subsequent results, because as long as we assume that the intruding magmas and the host rocks are of similar composition, any change in that composition will alter the densities of the host rocks and the magma by nearly the same fractional amounts, and so the ratio of the two densities, which is the main factor controlling the neutral buoyancy depth, will change only very slightly.

[12] We now define the likely conditions in a magma source feeding the giant dikes, assumed to be a mafic magma reservoir centered at the 10.3 km deep neutral buoyancy level of the magma that it contains. The depth to the top of the reservoir is D, and it has a half-height R so that the neutral buoyancy depth is $(D + R)$ and the bottom of the reservoir is at depth $(D + 2R)$. *Wilson and Head* [1994] argued that because the vertical stresses in planetary lithospheres scale with the gravity, whereas magma compressibilities and rock strengths are independent of gravity, the vertical extents of magma reservoirs were likely to be inversely proportional to the acceleration due to gravity, provided that they were completely contained within the lithosphere. The vertical extents of the reservoirs in basaltic volcanoes such as Kilauea and Mauna Loa are estimated, on the basis of seismic tomography, to be ~3.5 km [*Ryan*, 1988], and so we assume that the vertical extent of our Martian reservoir will be (9.8/3.74) times larger, i.e., 9.2 km, so that $R = 4.6$ km; the roof, middle, and floor of the reservoir are then at depths 5.7, 10.3, and 14.9 km, respectively.

[13] Earlier treatments of the conditions in magma reservoirs [*Tait et al.*, 1989; *Parfitt et al.*, 1993] have addressed the issue of the variation of magma density with depth due to volatile exsolution in various ways. Here we assume that the walls of the reservoir behave in an elastic fashion and that there is an excess pressure (i.e., one in addition to any hydrostatic pressure) P_e in the magma. By definition, P_e is the pressure in the magma immediately beneath the roof of the reservoir, which we show shortly is likely to be several tens of MPa. The magma bulk density ρ_m varies with depth

h below the roof of the reservoir because of the presence of the exsolved gases. By analogy with *Gerlach*'s [1986] study of the basaltic magma reservoir of Kilauea Volcano, Hawai'i, we assume initially that the Martian reservoir is fed by magma from the mantle that contains 0.3 mass% H_2O, 0.65 mass% CO_2, and 0.13 mass% S (we comment later on the consequences of changing the assumed initial volatile contents.). During its pre-eruption residence in the reservoir it loses some of the volatiles as the magma becomes supersaturated and bubbles of exsolved supercritical gas drift upward to the roof and are lost by seepage into the host rocks. The controlling volatile is CO_2 because this is the least soluble and so supersaturates first. Once it does so, small amounts of both H_2O and S are partitioned into the vapor phase and also lost, leaving a magma containing 0.27 mass% H_2O and 0.07 mass% S. The amount of residual CO_2 depends on the extent to which the magma in the reservoir undergoes vertical mixing, and hence exposure to the complete range of pressures within the reservoir, during its pre-eruption residence. The limits on the amount of residual CO_2 are therefore its solubility at the pressure at the roof of the reservoir, P_e, and at the pressure at the base. Because the pressure at the base is equal to the pressure at the roof plus the gravitational load of the intervening magma, and because the density of this magma itself depends on the amount of CO_2 exsolved, the calculation is not trivial.

[14] We therefore proceed by defining the pressure P_e at the top of the reservoir and then choosing a value for the pressure P_{sat} (by definition, greater than or equal to P_e) at which the CO_2 has become saturated. The solubility n_{dCO2} of CO_2 in typical basaltic (e.g., tholeiitic) magmas is given by [*Harris*, 1981; *Dixon*, 1997]

$$n_{dCO2} = 5.9 \times 10^{-12} P + 5.0 \times 10^{-6}, \quad (3)$$

where n_{dCO2} is expressed as a mass fraction and P is the pressure in Pascals. So, by setting P equal to P_{sat}, we define the total amount of CO_2 in the reservoir magma, n_{totCO2}, by

$$n_{totCO2} = 5.9 \times 10^{-12} P_{sat} + 5.0 \times 10^{-6}. \quad (4)$$

We then calculate the mass fraction of CO_2 exsolved at any pressure, P, less than P_{sat}, n_{eCO2}, from

$$n_{eCO2} = n_{totCO2} - n_{dCO2} \quad (5)$$

and calculate the bulk density of the magma, ρ_m, in the usual way from the partial volumes of the components,

$$1/\rho_m = [(n_{eCO2}\, Q\, T)/(m_{CO2}\, P)] + [(1 - n_{eCO2})/\rho_{ml}], \quad (6)$$

where Q is the universal gas constant (8.314 kJ kmol^{-1} K^{-1}), T is the magma temperature (say, 1470 K by analogy with terrestrial basalts), m_{CO2} is the molecular mass of CO_2, 44 kg kmol^{-1}, and ρ_{ml} is the density of the bubble-free mafic magmatic liquid, taken earlier as 2600 kg m^{-3}. It should be noted that although we assume that some H_2O is lost from the reservoir along with the equilibrating CO_2, we do not take account of the presence of this vapor in calculating the above magma bulk density. This is because, as shown by *Gerlach* [1986], the amount of H_2O vapor present at any time will be very small until the pressure decreases to a value approaching the saturation limit that would apply to H_2O if it were the only volatile present. The water-alone solubility is [*Dixon*, 1997]

$$n_{dH2O} = 6.8 \times 10^{-8} P^{0.7}, \quad (7)$$

where n_{dH2O} is expressed as a mass fraction and P is the pressure in Pascals. Thus, if 0.27 mass%, i.e., 0.0027 mass fraction, of water remains in the reservoir magma, then P must decrease to less than ~3.7 MPa before saturation occurs. This is an order of magnitude less than the minimum likely pressure in the reservoir, P_e. As we shall see later, exsolution of water becomes an issue only at the pressures relevant to the upper tip of any dike which is emplaced from the reservoir. Similar arguments appear to apply [*Gerlach*, 1986] to the release of volatiles involving S (in practice, mainly SO_2 at low pressures), and in fact we neglect the details of this in the present treatment on the grounds that the amounts of S present are likely to be significantly less than the amounts of H_2O.

[15] We perform the calculation of the magma bulk density first for the magma at the roof of the chamber, where we know that the pressure is $P = P_e$, and then obtain the pressure as a function of depth, h, below the roof of the reservoir by integrating downward numerically:

$$P(h + dh) = P(h) + \rho_m(h)\, g\, dh. \quad (8)$$

When $h = R$, we note the pressure on the centerline of the reservoir, P_c, and we terminate the process at the floor of the reservoir when h becomes equal to ($2R$), thus finding the pressure here, P_f. Table 2 shows some examples of the consequences of various plausible combinations of choices of P_e and P_{sat}, giving the internal reservoir pressures P_r, P_c, and P_f at the roof, center, and floor and also the corresponding differences, ΔP_r, ΔP_c, and ΔP_f, between the internal pressure and the external lithostatic host rock stress calculated from (2). If any of the ΔP values is so negative that its absolute value exceeds twice the tensile strength of the host rocks, the reservoir wall will fail in tension [*Tait et al.*, 1989] and a dike will begin to propagate away from the reservoir. If any of the ΔP values is sufficiently positive that it exceeds twice the compressive strength of the host rocks, the wall will fail in compression and pathways allowing gas loss to the surface may be initiated. Note that ΔP_c is always greater than either of ΔP_r or ΔP_f: this is generally true of pressurized magma reservoirs centered at neutral buoyancy levels [*Parfitt et al.*, 1993] and implies that failure of the reservoir walls is most likely to occur in compression at the depth of the reservoir center and in tension at the roof (and floor, if the host rocks behave elastically there).

[16] Table 2 shows that ΔP_r, ΔP_c, and ΔP_f depend strongly (and linearly) on P_e but are only weakly dependent on the exact amount of CO_2 exsolved as dictated by P_{sat} (the range covered in Table 2 spans a factor of ~4.5, from ~2×10^{-4} to ~9×10^{-4}, i.e., 0.02–0.09 mass%). If we assume that the host rock strengths are of order 5 MPa in tension and 10 MPa in compression [*Tait et al.*, 1989], then wall failure will occur if any of the values of ΔP is less than −10 MPa or greater than 20 MPa. Table 2 then shows that failure will occur at the roof if P_e is less than 33.1 MPa, and failure at the floor will occur if P_e is greater than 62.4 MPa. No stable reservoir of the size we have invoked could exist unless P_e lies between these values. Furthermore, the values of ΔP_c, since they represent the difference between the internal magma pressure and the external compressive stress at the neutral buoyancy level, are by definition the driving pressures which will control the propagation of any dikes that leave the reservoir. We assume, in saying this, that no deviatoric (i.e., nonhydrostatic) stresses act in the lithosphere and return to this issue in the next section. Since the driving pressure ΔP_c must necessarily be positive for a dike to propagate, we infer that P_e must in fact also be greater than ~41 MPa. The upper limit of ~62 MPa applies if the reservoir wall that fails in tension is smooth and has a large radius of curvature. Any irregularities in the wall will act as the foci of stress concentration and will allow the wall to fail at a smaller differential stress. We conclude at this stage that any value of P_e in the range ~41 to ~62 MPa is possible; the corresponding range of possible dike driving pressures is then 0 to ~21 MPa.

[17] We now use the values of P_c and ΔP_c to define the properties of a dike which has propagated laterally along the

Table 2. Pressure Distributions in a Typical Martian Magma Chamber[a]

P_e, MPa	P_{sat}, MPa	P_c, MPa	P_f, MPa	ΔP_r, MPa	ΔP_c, MPa	ΔP_f, MPa
35	35	83.6	132.2	−8.1	−6.1	−7.4
35	85	83.5	132.1	−8.1	−6.2	−7.5
35	130	83.4	131.9	−8.1	−6.4	−7.7
40	40	88.6	137.2	−3.1	−1.1	−2.4
40	88	88.5	137.1	−3.1	−1.2	−2.5
40	136	88.4	137.0	−3.1	−1.3	−2.7
45	45	93.6	142.2	2.0	3.9	2.6
45	93	93.5	142.1	2.0	3.8	2.5
45	141	93.4	142.0	2.0	3.7	2.3
50	50	98.6	147.2	7.0	8.9	7.6
50	98	98.5	147.1	7.0	8.8	7.5
50	147	98.4	147.0	7.0	8.7	7.3
55	55	103.6	152.2	12.0	13.9	12.6
55	103	103.5	152.1	12.0	13.8	12.5
55	152	103.4	152.0	12.0	13.7	12.3
60	60	108.6	157.2	17.0	18.9	17.6
60	108	108.5	157.2	17.0	18.8	17.5
60	159	108.4	157.0	17.0	18.7	17.4

[a] For various combinations of excess magma pressure, P_e, and pressure at which Co_2 is saturated, P_{sat}, in a magma reservoir with a vertical extent of 10 km centered at a depth of 10.3 km on Mars, values are given for P_c and P_f (the resulting pressures at the middle and floor of the reservoir, respectively), and ΔP_r, ΔP_c, and ΔP_f (the differences between the internal pressure and the external lithostatic host rock stress at the roof, middle and floor of the reservoir, respectively).

neutral buoyancy level from the reservoir into the surrounding host rocks. We assume for the moment that the topography at length scales of hundreds of kilometers is flat in order to avoid having to take account of gradients in magma pressure due to the slope of the neutral buoyancy level [*Fialko and Rubin*, 1999], which would be expected to lie at a fixed depth below the topographic surface. We also assume for the moment that the pressure conditions in the magma reservoir do not change as the dike propagates. This will be approximately true if the reservoir volume is much greater than the volume of the emplaced dike, but in general, the reservoir pressure will decrease as the dike is emplaced; we discuss the consequences of this later. Finally, the following calculation refers to the conditions in the dike after is has stopped propagating. While it is still being emplaced, there will be a pressure gradient acting laterally from the reservoir to the current location of the lateral dike tip in order to overcome the frictional and inertial forces associated with the magma motion, and so the vertical height of the dike above and below the neutral buoyancy level will be limited by the local value of the pressure at the dike center [*Lister*, 1990; *Rubin*, 1993a, 1993b]. As the lateral dike tip propagates to greater distances from the reservoir, the centerline pressure at any given location must increase with time, and so the dike must continue to grow vertically (unless it becomes trapped by the local stress regime) at all distances from the vent until the lateral tip ceases to move. The upward motion of the magma, like the lateral motion, is driven by a pressure difference, in this case the difference between the pressure on the dike centerline and the pressure at the upper dike tip (though part of this pressure difference, of course, simply supports the static weight of the magma column against gravity). The pressures at both the lateral dike tip and the upper dike tip cannot be arbitrarily small: they will be buffered, by the exsolution of H_2O vapor, at the saturation pressure of the magmatic water [*Rubin*, 1993a, 1993b], which, as we saw earlier from (7), is ~3.7 MPa for our assumed reservoir water content of 0.27 mass%. The reason for this buffering effect is that if the pressure decreases to a value significantly less than 3.7 MPa, water vapor is released from the magma adjacent to the tip to add to a growing gas pocket. This gas pocket will also contain, and in fact will probably be dominated by, carbon dioxide, because the magma which is immediately below the gas cavity must contain bubbles of carbon dioxide, some of which will burst through the interface and contribute gas to the cavity. As the lateral dike tip comes to rest, the pressure everywhere along the centerline equilibrates to the pressure on the centerline of the reservoir. At the same time, further upward growth occurs at all distances from the reservoir until a new equilibrium with the local stress regime is reached.

[18] In this final equilibrium the pressure along the upper edge of the dike is likely to remain close to 3.7 MPa, even though the pressure at the deeper, lateral tip has increased dramatically, compressing the gas pocket there. We argue this because the pressure in the upper dike tip will not have decreased to less than 3.7 MPa for the same reason that it did not do so while the dike was propagating. Also, it will not have increased to a larger value because if it did so the stress intensity at the upper tip of the dike would have increased and further upward propagation would have ensued. We use this pressure to find the half-height of the dike by carrying out the reverse of the process used to find the pressure on the centerline of the dike. Beginning from the centerline of the dike at depth $z = (R + D)$, where the pressure is P_c, we find the pressure change as z decreases by computing the magma bulk density from (6) and then finding

$$P(z - dz) = P(z) - \rho_m(z)\, g\, dz. \tag{9}$$

The upward integration is continued until the pressure 3.7 MPa is reached, and the value of z at which this happens, denoted Z, is recorded as the depth of the upper tip of the dike. The dike is then assumed to extend as far below the neutral buoyancy level as the upper tip extends above it. Values of Z are given in Table 3 for some of the same sets of permutations of P_e and P_{sat} that were used in Table 2. This time the choice is restricted to those values of P_e that led to positive values of ΔP_c, since only these correspond to the creation of dikes. It is found that Z decreases as P_e, and hence ΔP_c, increase. At $P_e = 45$ MPa, $\Delta P_c = 3.8$ MPa, Z is predicted to be 800–900 m. At $P_e = 50$ MPa, $\Delta P_c = 8.8$ MPa, Z is 300–400 m, and if $P_e = 55$ MPa, for which $\Delta P_c = 13.8$ MPa, Z becomes negative. In practice, this means that for P_e this large, magma extends all the way to the surface and erupts. Since we are looking for scenarios in which the dike intrudes to shallow depth but does not erupt, we conclude that we have further restricted the possible range of values of P_e: the lower limit is still set at ~41 MPa by the requirement that ΔP_c be positive, but now the need to have Z also be positive means that P_e should be no larger than ~53 MPa.

Table 3. Properties of a Dike Extending Laterally From a Typical Martian Magma Chamber[a]

P_e, MPa	P_{sat}, MPa	P_c, MPa	ΔP_c, MPa	Z, m	W, m	K_u, MPa m$^{1/2}$	L, m	n_{tH2O}	Z', m
45	45	93.6	3.9	926	32.1	124	2.1	1.8×10^{-9}	924
45	93	93.5	3.8	878	31.1	157	3.4	3.7×10^{-9}	875
45	141	93.4	3.7	831	30.0	182	4.6	6.0×10^{-9}	826
50	50	98.6	8.9	410	61.7	875	97	6.8×10^{-7}	313
50	98	98.5	8.8	357	61.0	909	104	7.6×10^{-7}	253
50	147	98.4	8.7	305	60.0	937	111	8.5×10^{-7}	194
55	55	103.6	13.9	−112	93.2	1660	316	4.1×10^{-6}	−528
55	103	103.5	13.8	−162	92.2	1693	329	4.4×10^{-6}	−491
55	152	103.4	13.7	−210	90.8	1720	340	4.7×10^{-6}	−550

[a] For a subset of the combinations given in Table 2 of excess magma pressure, P_e, and pressure at which CO_2 is saturated, P_{sat}, in a magma reservoir with a vertical extent of 10 km centered at a depth of 10.3 km on Mars, values are given for P_c and ΔP_c (the absolute pressure and the driving pressure on the centerline of the dike, respectively), Z (the depth below the surface of the top of the magma in the dike), W (the mean dike width), K_u (the stress intensity at the upper dike tip if the gas-filled cavity is ignored), L (the length of the gas-filled cavity), n_{tH2O} (the ratio of the mass of gas in the cavity to the mass of magma in the underlying dike) and Z' (the depth below the surface of the top of the dike).

[19] The next step in the analysis is to find the mean width of the dike, W. For the geometry considered here, *Rubin and Pollard* [1987] give

$$W = [(1-\upsilon)/\mu\}][0.5\ \pi\ \alpha_1\ \Delta P_c\, A - 0.33\, A^2\, g \cdot \{\alpha_2(\rho_{mt}-\rho_t) + \alpha_3(\rho_b-\rho_{mb})\}], \quad (10)$$

where A is the half-height of the dike; υ and μ are the Poisson's ratio and shear modulus of the country rocks, respectively; α_{1-3} are correction factors to take account of the proximity of the free surface; ρ_{mt} and ρ_{mb} are the mean density of the reservoir magma in the top half and the bottom half of the reservoir, respectively; and ρ_t and ρ_b are the corresponding average values of the density of the adjacent lithosphere, averaged over the same depth range. All of the densities are available via (1) and (6). Suitable values of υ and μ at shallow crustal depths are ~0.25 and ~3 GPa [*Parfitt*, 1991], though μ must be thought of as an effective value which is dependent on the physical state of the rocks and increases with depth [*Rubin*, 1993b]. For the present geometry, where the depth to the top of the dike is about one tenth of the depth to the neutral buoyancy zone, data given by *Rubin and Pollard* [1987] show that α_1 = ~1.38, α_2 = ~1.52, and α_3 = ~1.22. Using these parameters, we find the values of W given in Table 3. These are ~10, 33, and 62 m for P_e = 45, 50, and 55 MPa, respectively. These widths are significantly smaller than the values inferred from the measured graben properties; we return to this issue in section 4.

[20] The final important parameter which we can infer for the dike is the stress intensity K_u at its upper tip. This quantity is important because it is generally assumed that a dike will cease to propagate when the stress intensity at its tip is equal to a quantity called the fracture toughness K_c [*Secor and Pollard*, 1975]. The stress intensity at the upper tip of a dike centered on the neutral buoyancy zone which is full of magma is given by *Rubin and Pollard* [1987] as

$$K_u = \beta_1\ \Delta P_c\, A^{1/2} - \left[\left(\pi^{-1}+4^{-1}\right)\beta_2(\rho_{mt}-\rho_t) - \left(\pi^{-1}-4^{-1}\right)\beta_3(\rho_b-\rho_{mb})\right] g\, A^{3/2}, \quad (11)$$

where the factors β_{1-3}, like the factors α_{1-3} in (10), are again correction factors to take account of the proximity of the free surface. *Rubin and Pollard* [1987] show that β_1 = ~1.65, β_2 = ~1.43, and β_3 = ~2.85 are suitable values. Table 3 shows the values calculated for P_e = 45, 50, and 55 MPa; they range from ~150 to ~1700 MPa m$^{1/2}$. The interpretation of these values is not trivial. *Rubin* [1993a] showed that fracture toughness is not a fundamental material property but is instead a function of the tensile strength, the mineralogical fabric scale, and the ambient stress conditions. The values of K_u found for the upper tips of laterally propagating dikes at Kilauea Volcano, Hawai'i, are ~100 MPa m$^{1/2}$ [*Parfitt*, 1991], to be compared with measured zero-stress values, which are always less than 10 MPa m$^{1/2}$ [*Rubin*, 1993a]. *Pollard* [1987] recognized that the large values inferred from assuming a dike to be full of magma all the way to its tip could be readily accounted for by realizing that a gas pocket in the tip would change the stress conditions dramatically. In terms of the notation used here, he showed that the presence of a gas cavity of length L would reduce the value of K_u found from (11) by an amount K_{diff}, where

$$K_{diff} = P_c\left[(8\,L)/\pi^2\right]. \quad (12)$$

[21] Table 3 shows the values of L required to reduce the values of K_u calculated from (11) to a nominal value of K_c = 3 MPa m$^{1/2}$; the values of L would be essentially the same for any assumed value of K_c less than 10 MPa m$^{1/2}$. In order to assess the significance of the values of L required, we give in the penultimate column of Table 3 the mass fraction n_{tH2O} of the magma in the dike which is represented by the mass of gas contained in the dike tip cavity at the buffered pressure of 3.7 MPa assuming that the gas is entirely H_2O. The cross-sectional area of the gas-filled dike tip is found by expanding the equations for dike shapes given by *Weertman* [1971] in terms of distance measured from the dike tip. For the present case, in which the magma is negatively buoyant in the upper half of the dike and L is always much less than A, this implies that the width of the base of the cavity is equal to $\{[(1-\upsilon)/\mu]\ \Delta P_c\ [8\,A\,L]^{1/2}\}$, and the cavity area is then $\{[(1-\upsilon)/\mu]\ (2/3)\ \Delta P_c\ [8\,A\,L^3]^{1/2}\}$. The gas density is computed from the 3.7 MPa pressure via the perfect gas law assuming that the gas is at the same 1470 K temperature as the magma and the mean magma density is obtained by averaging the local magma density as a function of depth over the entire vertical extent of the dike which contains magma. Table 3 shows that all of the values of n_{tH2O} are less than ~5×10^{-6}. It will be recalled that our model assumes that the magma contains 0.27 mass% H_2O, i.e., a mass fraction of 0.0027; thus, at the very most only two thousandths of the water contained in the magma in the dike needs to be exsolved in order to justify the size of the gas-filled cavity implied here. If we assume that the gas in the cavity is entirely CO_2, the equivalent calculation implies that the mass fraction of CO_2 in the dike magma needed to populate the cavity is less than ~10^{-5}; comparing this with the actual CO_2 content of the magma, between 3 and 9×10^{-4}, we find that no more than ~3% of the available CO_2 would be needed. The final column of Table 3 shows the result of adding the length of the gas-filled cavity to the length of the magma-filled part of the dike and thus finding the final estimate Z' of the depth of the dike top below the surface. This allows a final, small additional narrowing down of the range of allowed models: if Z' is to be positive, i.e., the magma is not to erupt, clearly P_e must be no more than ~52 MPa. Of course, if we wish the dike top to be some hundreds of meters below the surface, as was implied by our

analysis of the graben geometry (penultimate column of Table 1), P_e is even more restricted, to being no more than ~50 MPa.

[22] All of the numerical values quoted above correspond to the assumed residual reservoir magma water content of 0.0027 mass fraction. To explore the sensitivity of the model to this value, we have repeated all of the calculations for a wide range of water contents, from negligibly small to 0.02, i.e., 2 mass%, a little greater than the largest value yet inferred for melts from the Martian mantle [*Minitti and Rutherford*, 2000]. The net effect of increasing the water content is to place the upper dike tip at a greater depth below the surface, and so it is reductions in water content that matter most. As a typical illustration, in order for the dike tip not to reach the surface when the water content is reduced by a factor of 2, to 0.00135, the required value of P_e is reduced from ~52 MPa to ~50 MPa; the effect is not large. The consequence for the calculated mean dike widths of changing the magma water content across the above range is extremely small, no more than a few percent.

[23] We close this section by noting that we have not addressed the issue of the stress intensity at the bottom edge of the dike. This is because the host rocks are much hotter at the 20 km depth of the root of the dike than near the surface and are much less likely to behave in a purely elastic fashion [*Dyer*, 1998]. This might be particularly true in the case of the region around Alba Patera if, as suggested by *McGovern et al.* [1999], the Alba Patera edifice was underplated with a buoyant residuum late in its lifespan or, as argued by *Scott* [2000a, 2000b], this region underwent convective removal of its lithospheric root with replacement by hotter mantle material. Under these circumstances the relationships between dike geometry and internal pressure distribution begin to depend to an important extent on the ratio of the plastic viscosity of the host rocks to the apparent viscosity of the dike magma [*Rubin*, 1993b]. Treatment of these issues is beyond the scope of the present analysis.

4. Discussion

[24] The above analysis shows that it is possible to produce a model of laterally propagating, ~20 km high elastic dikes which have the expected property of being trapped with their centers at the ~10 km deep neutral buoyancy level and the required property of not extending any closer to the surface than a few hundreds of meters. However, the model predicts mean dike widths of at most ~60 m (values of W in Table 3), whereas the geometries of the graben (Table 1) imply dike widths of ~65–405 m if we base these on the graben extensions and ~130–440 m if we use the graben depths. A possible explanation of this discrepancy is clearly that any one graben represents the accumulated response of the crust to the intrusion of more than one dike. Indeed, the relatively complex nature of the fractures associated with some of the graben (see Figure 2) suggests that this is in fact the correct explanation in some cases. However, the roughly north-south propagation direction of all of the giant dikes and their spatial distribution around the Alba Patera edifice (Figure 1) make it clear that at the time of their emplacement the large-scale extensional stress fields associated with the arcuate Alba graben and the linear graben to the south of Alba were still in existence, and we now show how the presence of such stress fields can explain the apparent dike width anomaly.

[25] This stress regime can be accommodated into the dike model by regarding it as a horizontally oriented tensile stress deviator T and modifying the driving stress controlling the dike by adding the absolute value of T to ΔP_c [e.g., *Rubin and Pollard*, 1987]. Increasing the dike driving pressure in this way has no effect on the minimum value deduced for the magma reservoir excess pressure, since that value was derived from the radial stress at the reservoir roof (or floor), but would decrease the maximum value of excess pressure required. Adding to the driving pressure in this way would also increase the mean width of the dike, but only at the expense of increasing the size of the gas-filled cavity required to trap the upper tip of the dike below the surface. It is easy to show that doubling the dike width would require the gas cavity size to be approximately doubled. Any increase in the size of the gas-filled cavity would further reduce the upper limit allowed for P_e, which would in itself decrease the implied dike width.

[26] These complex relationships are best illustrated by an example. The extensions across graben G1–G3 are of order 100–300 m (Table 1). If we assume that the extension across any one of these graben represents the relief of a tensile stress which has accumulated across the east-west extent of the entire region occupied by the volcanic graben, which Figure 1 shows to be ~1000 km, the strain represented is $\sim 1-3 \times 10^{-4}$. Using a Young's modulus of ~70 GPa [*Turcotte and Schubert*, 1982, p. 432], this implies a tensile stress of ~7–21 MPa. Now consider the entries in Table 3 for P_e = 50 MPa and P_{sat} = 98 MPa. The dike driving pressure, ΔP_c, is just less than 9 MPa, producing a dike width of W = ~61 m and a gas cavity length of L = ~104 m, in turn placing the dike tip $Z' = (Z - L) = (357 - 104) = 253$ m below the surface. If we now add the value T = 5 MPa to the driving pressure, so that ΔP_c = 14 MPa, we find a new mean dike width of ~(14/9) × 61 = ~95 m, a gas cavity length of ~(14/9) × 104 = ~162 m, and a dike tip located (357 − 162) = 195 m below the surface. If we repeat this process with T = 15 MPa, we find ΔP_c = ~24 MPa, W = ~(24/9) × 61 = 163 m, L = ~(24/9) × 104 = ~277 m, and a dike tip located (357 − 277) = 80 m below the surface. The dike widths just calculated, 95–163 m, more than include the complete range of dike widths inferred in Table 1 for the dikes beneath graben G1 and G2, and the scenarios they represent all involve dikes which intrude but do not break though to the surface, as required. Thus the formation of these graben above dikes emplaced while a regional tension of 5–15 MPa was in existence would be self-consistent.

[27] In the case of the graben G3, it would be necessary to invoke either a somewhat greater regional tension or some degree of inelastic extension across the graben not linked directly to the dike emplacement or both. Regional tensions greater than ~22 MPa would lead to model solutions in which the dike reached the surface. This limit could be changed somewhat by starting the illustration with a different value of P_e or P_{sat}. For example, if a regional tension T = 30 MPa is applied to the model in Table 3 with P_e = 45 MPa, a mean dike width of 275 m is produced with the dike top still 848 m beneath the surface, and much larger tensions would be allowed before the dike top reached the surface. Given the uncertainties in the relationships between dike emplacement and graben formation, we are satisfied that some geologically plausible permutation of magma reservoir conditions and regional stress configuration can explain all of the volcanic graben shown in Figure 1.

5. Inferences for the Dike Magma Source Reservoir

[28] We showed in section 2 that the magma source which spawned the giant dikes was active immediately after the eruptive life of Alba Patera and during its period of tectonic adjustment. It is possible that this magma source was a low-angle shield volcano like Alba Patera or, indeed, that it was a crustal intrusion with little or no positive surface expression. It is certainly much more difficult to argue that it was a Tharsis Montes—type shield volcano, because we would have to argue that all evidence of its proximal products is buried beneath the younger, current Tharsis Montes volcanoes and Olympus Mons, leaving no indication of its existence. We attempt to clarify the issue by considering the volume of a reservoir which might have given rise to the giant dike swarm.

[29] The volume of magma contained in any one of the giant dikes can be estimated from the length, ~1000 km, the mean horizontal width, ~100 to ~400 m, depending on the criterion used to estimate the width (see Table 1), and the vertical extent,

~20 km, to be ~2000 to ~8,000 km^3. If this were the result of the deflation of a magma reservoir that had inflated and then subsequently relaxed, in a purely elastic fashion, the maximum amount of magma that it would discharge would be ~0.3% of its volume [*Blake*, 1981]. To supply a 2000–10,000 km^3 dike volume would therefore require a reservoir volume of ~0.7–3.3 × 10^6 km^3. This can be compared with the volume estimates for the existing magma reservoirs of, e.g., the Tharsis volcanoes. The diameters of three of the eight well-defined calderas at the summit of Olympus Mons are 20, 40, and 60 km; that of the single large Arsia Mons caldera is 100 km. This size range encompasses all of the other major Martian calderas. Assuming that each of these calderas marks the location of a magma reservoir with a vertical height of order 10 km [*Wilson and Head*, 1994], the implied reservoir volumes are close to 3000, 10,000, 30,000, and 10^5 km^3, respectively. None of these approaches the value of ~10^6 km^3 required to feed a giant dike by purely elastic deformation of the reservoir. We therefore turn to the possibility that magma was expelled from a reservoir in a different way.

[30] One possibility is that as magma was removed from the reservoir, the internal pressure decreased to the point where the reservoir roof failed and caldera collapse occurred. The simplest way to illustrate this is to calculate the vertical amount of collapse needed for each of the four reservoir diameters quoted above: 20, 40, 60, and 100 km. The corresponding subsidence distances required to provide the larger estimate of the dike volume, 8,000 km^3, are ~26, 6, 3, and 1 km; to provide the smaller dike volume estimate, 2000 km^3, the values are ~6, 1.6, 0.8, and 0.25 km. The actual depths of the Tharsis calderas range from less than 1 to at least 3 km [*Crumpler et al.*, 1996]. We therefore conclude that collapse events in reservoirs similar to all but the smallest of the most recent Tharsis magma reservoirs could have liberated large enough magma volumes to create (single) giant dikes. A 3 km subsidence of the roof of a reservoir the size of that under the summit of Arsia Mons could feed several such dikes in a single event.

[31] A second possible way to avoid the limitations of elastic reservoir response is to assume that the reservoir feeding the giant dikes was itself fed with magma from a deeper source during a period of enhanced partial melting in the mantle [*Wilson et al.*, 2001]. The pressure conditions in the reservoir would then be dictated by the relative rates of magma input from below and output into the currently growing dike and under a wide range of conditions could be buffered at a near-constant value [*Parfitt and Head*, 1993]. This eruption process need not involve caldera collapse or any other surface indication of the event.

6. Conclusions

1. A system of at least 4–6 giant dikes, radiating from a source ~1000 km to the south in central Tharsis, produced a series of volcanic graben which intersect the mainly circumferential and the more nearly linear regional tectonic graben associated with the Alba Patera shield volcano.

2. The giant dikes inferred to have produced the volcanic graben appear to have propagated laterally with their centers coincident with the level of neutral buoyancy of the magma they contain. Their vertical extents and the depth of their upper edges are consistent with the pressures and stresses expected in a feeding reservoir also centered at the neutral buoyancy level provided that a small amount of carbon dioxide was exsolved from the magma in the upper tip of the dike to form a gas cavity.

3. The widths of the dikes implied by the geometries of the narrower graben are consistent with a causative link between dike emplacement and extension across the graben and correspond to the relaxation of regional extensional tectonic stresses of a few tens of MPa which were responsible for the roughly north-south orientation of the giant dikes.

4. The volume of magma contained in each of the giant dikes was ~2000–8000 km^3. Volumes this large could not plausibly be released from a magma reservoir acting elastically unless its volume were at least an order of magnitude larger than that of any reservoir for which there is currently evidence on Mars. Such volumes could, however, easily be released from plausible reservoirs if the intrusions coincided with caldera collapse events similar to those implied by the depths of presently observable calderas on Martian shield volcanoes or if the reservoir conditions were buffered during the intrusion by a period of enhanced magma supply from the mantle.

Notation

A	half-height of dike, m
D	depth to top of magma reservoir, equal to 5257, m
K_u	stress intensity at upper dike tip, Pa m$^{1/2}$
P	pressure in magma reservoir, Pa
P_{atm}	atmospheric pressure, equal to 600, Pa
P_c	pressure at center of magma reservoir, Pa
P_e	excess pressure in magma reservoir, Pa
P_f	pressure at floor of magma reservoir, Pa
P_l	lithostatic pressure, Pa
P_{sat}	pressure at which gas is just saturated in reservoir magma, Pa
Q	universal gas constant, equal to 8.31, kJ kmol^{-1} K^{-1}
T	temperature of magma, equal to 1470, K
R	half-height of magma reservoir, equal to 5, km
V_0	surface rock volume fraction consisting of void space, equal to 0.3
W	mean width of dike, m
Z	depth of upper tip of dike below surface, m
g	acceleration due to gravity, equal to 3.74, m s^{-2}
h	depth below roof of reservoir, m
m_{CO2}	molecular mass of CO_2, equal to 44 kg kmol^{-1}
m_{H2O}	molecular mass of H_2O, equal to 18 kg kmol^{-1}
n_{dCO2}	solubility of CO_2 in basaltic magma, mass fraction
n_{dH2O}	solubility of H_2O in basaltic magma, mass fraction
n_{eCO2}	amount of CO_2 exsolved from reservoir magma, mass fraction
n_{totCO2}	amount of CO_2 dissolved in reservoir magma, mass fraction
z	depth below the surface, m
ΔP_c	outward stress across reservoir wall at centerline, Pa
ΔP_e	outward stress across reservoir wall at roof, Pa
ΔP_f	outward stress across reservoir wall at floor, Pa
α_{1-3}	correction factors for presence of free surface, equal to 1.38, 1.52, and 1.22
β_{1-3}	correction factors for presence of free surface, equal to 1.65, 1.43, and 2.85
λ	void space decay constant, equal to 1.18 × 10^{-8}, Pa^{-1}
ρ_l	density of the lithosphere, kg m^{-3}
ρ_m	bulk density of vesicular magma, kg m^{-3}
ρ_{mb}	mean density of magma in bottom half of reservoir, kg m^{-3}
ρ_{mt}	mean density of magma in top half of reservoir, kg m^{-3}
ρ_b	mean lithosphere density over bottom half of reservoir, kg m^{-3}
ρ_t	mean lithosphere density over top half of reservoir, kg m^{-3}
ρ_∞	density of void-free lithospheric rocks, equal to 2900, kg m^{-3}

[32] **Acknowledgments.** This work was supported in part by NASA grants NAG5-10690 and NAG5-9780 to J.W.H. and in part by PPARC grant PPA/G/S/2000/00521 to L.W. We thank Larry Mastin for his constructive comments on this paper and are particularly grateful to Daniel

Mège for his detailed and insightful review discussing the limitations of current models of graben formation.

References

Blake, S., Volcanism and the dynamics of open magma chambers, *Nature*, *289*, 783–785, 1981.

Cattermole, P., *Planetary Volcanism: A Study of Volcanic Activity in the Solar System*, John Wiley, New York, 1996.

Crumpler, L. S., J. W. Head, and J. C. Aubele, Calderas on Mars: Characteristics, structure and associated flank deformation, in *Volcano Instability on the Earth and Other Planets*, edited by W. J. McGuire, A. P. Jones, and J. Neuberg, *Geol. Soc. Spec. Publ.*, *110*, 307–348, 1996.

Dixon, J. E., Degassing of alkali basalts, *Am. Mineral.*, *82*, 368–378, 1997.

Dyer, N., An investigation into the mechanism of ascent of mafic magma through the lithosphere of the Earth, Ph.D. thesis, 293 pp., Lancaster Univ., Lancaster, U.K., 1998.

Ernst, R. E., J. W. Head, E. Parfitt, E. Grosfils, and L. Wilson, Giant radiating dike swarms on Earth and Venus, *Earth Sci. Rev.*, *39*, 1–58, 1995.

Fialko, Y. A., and A. M. Rubin, What controls the along-strike slopes of volcanic rift zones, *J. Geophys. Res.*, *104*, 20,007–20,020, 1999.

Gerlach, T. M., Exsolution of H_2O, CO_2, and S during eruptive episodes at Kilauea Volcano, *Hawaii, J. Geophys Res.*, *91*, 12,177–12,185, 1986.

Golombek, M. P., The Mars Pathfinder Mission, *Sci. Am.*, *279*(1), 24–33, 1998.

Golombek, M. P., K. L. Tanaka, and B. J. Franklin, Extension across Tempe Terra, Mars, from measurements of fault scarp widths and deformed craters, *J. Geophys. Res.*, *101*, 26,119–26,130, 1996.

Gudmundsson, A., Form and dimensions of dykes in eastern Iceland, *Tectonophys.*, *95*, 295–307, 1983.

Harris, D. M., The concentration of CO_2 in submarine tholeiitic basalts, *J. Geol.*, *89*, 689–701, 1981.

Head, J. W., and L. Wilson, Magma reservoirs and neutral buoyancy zones on Venus: Implications for the formation and evolution of volcanic landforms, *J. Geophys. Res.*, *97*, 3877–3903, 1992.

Head, J. W., and L. Wilson, Lunar graben formation due to near surface deformation accompanying dike emplacement, *Planet. Space Sci.*, *41*, 719–727, 1993.

Head, J. W., N. Seibert, S. Pratt, D. Smith, M. Zuber, J. B. Garvin, and P. J. McGovern, Volcanic calderas on Mars: Initial views using Mars Orbiter Laser Altimetry data (abstract), *Lunar Planet. Sci.* [CD-ROM], *XXIX*, 1488, 1998.

Hodges, C. A., and H. J. Moore, Atlas of volcanic landforms on Mars, *U.S. Geol. Surv. Prof. Pap.*, *1534*, 1994.

Lister, J. R., Buoyancy-driven fluid fracture: Similarity solutions for the horizontal and vertical propagation of fluid-filled cracks, *J. Fluid. Mech.*, *217*, 213–239, 1990.

Mastin, L. G., and D. D. Pollard, Surface deformation and shallow dike intrusion processes at Inyo Craters, Long Valley, California, *J. Geophys. Res.*, *93*, 13,221–13,235, 1988.

McGovern, P. J., S. C. Solomon, S. E. Faulkner, J. W. Head, D. E. Smith, and M. T. Zuber, Extension and volcanic loading at Alba Patera: Insights from MOLA observations and loading models (abstract), *Lunar Planet. Sci.* [CD-ROM], *XXX*, 1697, 1999.

McSween, H. Y., et al., Chemical, multi-spectral, and textural constraints on the composition and origin of rocks at the Mars Pathfinder landing site, *J. Geophys. Res.*, *104*, 8679–8715, 1999.

Mège, D., and P. Masson, A plume tectonics model for the Tharsis Province, Mars, *Planet. Space Sci.*, *44*, 1499–1546, 1996a.

Mège, D., and P. Masson, Amounts of crustal stretching in Valles Marineris, Mars, *Planet. Space Sci.*, *44*, 749–782, 1996b.

Minitti, M. E., and M. J. Rutherford, Genesis of the Mars Pathfinder "sulfur-free" rock from SNC parental liquids, *Geochim. Cosmochim. Acta*, *64*, 2535–2547, 2000.

Parfitt, E. A., The role of rift-zone storage in controlling the site and timing of eruptions and intrusions of Kilauea Volcano, Hawaii, *J. Geophys. Res.*, *96*, 10,101–10,112, 1991.

Parfitt, E. A., and J. W. Head, Buffered and unbuffered dike emplacement events on the Earth and Venus: Implications for the magma reservoir size, depth, and rate of replenishment, *Earth Moon Planets*, *61*, 249–281, 1993.

Parfitt, E. A., L. Wilson, and J. W. Head, Basaltic magma reservoirs: Factors controlling their rupture characteristics and evolution, *J. Volcanol. Geotherm. Res.*, *55*, 1–14, 1993.

Pollard, D. D., Elementary fracture mechanics applied to the structural interpretation of dikes, in *Mafic Dike Swarms*, edited by H. C. Halls and W. F. Fahrig, *Geol. Assoc. Can. Spec. Pap.*, *34*, 5–24, 1987.

Rubin, A. M., Dike-induced faulting and graben subsidence in volcanic rift zones, *J. Geophys. Res.*, *97*, 1839–1858, 1992.

Rubin, A. M., Tensile fracture of rock at high confining pressure: Implications for dike propagation, *J. Geophys. Res.*, *98*, 15,919–15,935, 1993a.

Rubin, A. M., Dikes vs. diapirs in viscoelastic rock, *Earth Planet. Sci. Lett.*, *119*, 641–659, 1993b.

Rubin, A. M., and D. D. Pollard, Origins of blade like dikes in volcanic rift zones, in *Volcanism in Hawaii*, *U.S. Geol. Surv. Prof. Pap.*, *1350*, chap. 53, pp. 1449–1470, 1987.

Ryan, M. P., Neutral buoyancy and the mechanical evolution of magmatic systems, *Spec. Publ. Geochem. Soc.*, *1*, 259–284, 1987.

Ryan, M. P., The mechanics and three-dimensional internal structure of active magmatic systems: Kilauea Volcano, Hawaii, *J. Geophys. Res.*, *93*, 4213–4248, 1988.

Scott, E. D., Sub-lithospheric subduction on Mars: Convective removal of a lithospheric root, I, The mechanism (abstract), *Lunar Planet. Sci.* [CD-ROM], *XXXI*, 1246, 2000a.

Scott, E. D., Sub-lithospheric subduction on Mars: Convective removal of a lithospheric root, II, Alba Patera (abstract), *Lunar Planet. Sci.* [CD-ROM], *XXXI*, 1329, 2000b.

Scott, E. D., and L. Wilson, Plinian eruptions and passive collapse events as mechanisms of formation for Martian pit chain craters, *J. Geophys. Res.*, *107*(E4), 10.1029/2000JE001432, 2002.

Secor, D. T., and D. D. Pollard, On the stability of open fractures in the Earth's crust, *Geophys. Res. Lett.*, *2*, 510–513, 1975.

Smith, D. E., et al., Topography of the northern hemisphere of Mars from the Mars Orbiter Laser Altimeter, *Science*, *279*, 1686–1692, 1998.

Smith, D. E., et al., Mars Orbiter Laser Altimeter (MOLA): Experiment summary after the first year of global mapping of Mars, *J. Geophys. Res.*, *106*, 23,689–23,722, 2001.

Srnka, L. J., J. L. Hoyt, J. V. S. Harvey, and J. E. McCoy, A study of the Rima Sirsalis lunar magnetic anomaly, *Phys. Earth Planet. Inter.*, *20*, 281–290, 1979.

Tait, S. R., C. Jaupart, and S. Vergniolle, Pressure, gas content and eruptive periodicity of a shallow magma chamber, *Earth. Planet. Sci. Lett.*, *92*, 107–123, 1989.

Tanaka, K. L., Tectonic history of the Alba Patera-Ceraunius Fossae region of Mars, *Proc. Lunar Planet. Sci. Conf. 20th*, 515–523, 1990.

Tanaka, K. L., and M. P. Golombek, Martian tension fractures and the formation of grabens and collapse features at Valles Marineris, *Proc. Lunar Planet. Sci. Conf. 19th*, 383–396, 1989.

Turcotte, D. L., and G. Schubert, *Geodynamics: Application of Continuum Physics to Geological Problems*, 450 pp., John Wiley, New York, 1982.

Turtle, E. P., and H. J. Melosh, Stress and flexural modelling of the Martian lithospheric response to Alba Patera, *Icarus*, *126*, 197–211, 1997.

Weertman, J., Theory of water-filled crevasses in glaciers applied to vertical magma transport beneath oceanic ridges, *J. Geophys. Res.*, *76*, 1171–1183, 1971.

Wilson, L., and J. W. Head, Mars: Review and analysis of volcanic eruption theory and relationships to observed landforms, *Rev. Geophys.*, *32*, 221–263, 1994.

Wilson, L., and J. W. Head, Tharsis-radial graben systems as the surface manifestation of plume-related dike intrusion complexes: Models and implications, *J. Geophys. Res.*, in press, 2002.

Wilson, L., and E. A. Parfitt, Widths of dikes on Earth and Mars (abstract), *Lunar Planet. Sci.*, *XXI*, 1345–1346, 1990.

Wilson, L., J. W. Head, and E. A. Parfitt, The relationship between the critical height of a volcano and the depth to its magma source zone: A critical reexamination, *Geophys. Res. Lett.*, *19*, 1395–1398, 1992.

Wilson, L., E. D. Scott, and J. W. Head, Evidence for episodicity in the magma supply to the large Tharsis volcanoes, *J. Geophys. Res.*, *106*, 1423–1434, 2001.

J. W. Head III, Department of Geological Sciences, Brown University, Box 1846, Providence, RI 02912, USA. (james_head_III@brown.edu)

E. D. Scott and L. Wilson, Environmental Science Department, Institute of Environmental and Natural Sciences, Lancaster University, Lancaster LA1 4YQ, UK. (l.wilson@lancaster.ac.uk)